Science of the Total Environment 980 (2025) 179565

Contents lists available at ScienceDirect

Science of the Total Environment

journal homepage: www.elsevier.com/locate/scitotenv

Earlywood vessel characteristics are early indicators of drought-induced decline in ring-porous oak species within the Mediterranean Basin

Michele Colangelo [a,*], Antonio Gazol [b], J. Julio Camarero [b], Marco Borghetti [a], Raúl Sánchez-Salguero [c], Luis Matias [d], Maria Castellaneta [a], Paola Nola [e], Francesco Ripullone [a]

[a] Dipartimento di Scienze Agrarie, Forestali, Alimentari ed Ambientali, Università degli Studi della Basilicata, 85100 Potenza, Italy
[b] Instituto Pirenaico de Ecología (IPE-CSIC), Avda. Montañana 1005, 50192 Zaragoza, Spain
[c] Departamento de Sistemas Físicos, Químicos y Naturales, Universidad Pablo de Olavide, 41013 Sevilla, Spain
[d] Departamento de Biología Vegetal y Ecología, Universidad de Sevilla, 41012 Sevilla, Spain
[e] Dipartimento Scienze della Terra e dell'Ambiente, Università degli Studi di Pavia, 27100 Pavia, Italy

HIGHLIGHTS

- Earlywood anatomy can serve as a valuable early-warning signals of oak decline.
- Growth rates differed between vigor classes 10 to 40 years before decay.
- Dieback is preceded by decline of vessel area dispersion decades earlier.
- Dispersion and spatial arrangement metric differentiates trees based on vigor class
- Different responses between vigor classes can explain physiological adjustments reflected in wood anatomy.

GRAPHICAL ABSTRACT

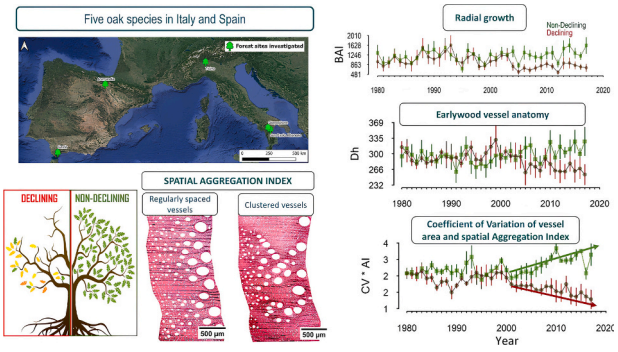

ARTICLE INFO

Editor: Manuel Esteban Lucas-Borja

Keywords:
Climate change
Quercus
Xylem
Vessel area
Vessel distribution
Earlywood anatomy

ABSTRACT

Heat and drought stress have triggered forest dieback episodes worldwide, affecting oak forests, particularly in hotspots of climate change such as the Mediterranean Basin. However, forecasting dieback is not straightforward. In this study, we used the earlywood anatomy to improve dieback forecasts in five oak species characterized by different drought sensitivity (i.e. from high to low *Quercus robur*, *Q. cerris*, *Q. frainetto* and *Q. canariensis*, *Q. humilis*, *Q. pubescens*) across Italy and Spain. We measured radial growth, expressed as basal area increment (BAI), earlywood hydraulic diameter (*Dh*) and vessel area of coexisting non-declining (ND) and declining (D) trees in each stand. Then, we calculated the product between the coefficient of variation (CV) of vessel area and a spatial aggregation index (AI). High CV × AI values indicate regularly spaced vessels with variable area of vessels, while low values correspond to clustered vessels with similar area. ND trees showed higher BAI values than D trees from 10 to 40 years before the dieback onset, when ND trees grew 20–50 % more than the D trees. We observed a decline in the vessel area CV several decades prior to dieback in D trees, with the exception of

* Corresponding author.
E-mail addresses: michele.colangelo@unibas.it (M. Colangelo), agazol@ipe.csic.es (A. Gazol), jjcamarero@ipe.csic.es (J.J. Camarero), marco.borghetti@unibas.it (M. Borghetti), rsanchez@upo.es (R. Sánchez-Salguero), lmatias@us.es (L. Matias), maria.castellaneta@unibas.it (M. Castellaneta), paola.nola@unipv.it (P. Nola), francesco.ripullone@unibas.it (F. Ripullone).

https://doi.org/10.1016/j.scitotenv.2025.179565
Received 3 January 2025; Received in revised form 25 April 2025; Accepted 28 April 2025
Available online 3 May 2025

Q. cerris. The AI showed higher values in ND than in D trees. Consequently, the CV × AI product was consistently higher in ND than in D trees. The CV × AI divergence between ND and D trees was pronounced in the wettest sites, specifically for *Q. robur* and *Q. humilis*. Time series of CV × AI effectively differentiated trees based on their vigor. Wood anatomy variables could be used to enhance predictions of vulnerability to drought-induced dieback. This study can help identify vulnerable trees before the onset of dieback symptoms, serving as a tool to support the management of forests prone to drought.

1. Introduction

Forests experiencing drought-induced dieback serve as valuable natural laboratories for identifying potential factors that trigger growth decline and for determining vulnerability thresholds (Allen et al., 2010; Camarero et al., 2015; Sánchez-Salguero et al., 2017; DeSoto et al., 2020; Preisler et al., 2021). The assessment of forest vulnerability to dieback is not straightforward due to the complex interactions of factors that influence the response of trees to climate stress. For this reason, some studies have used proxies of dieback such as crown defoliation, tree growth and wood anatomy data to assess changes in tree vigor (e.g. Pellizzari et al., 2016; Colangelo et al., 2017a, 2017b; Camarero et al., 2021; Valeriano et al., 2021a; Valeriano et al., 2021b; Castellaneta et al., 2022).

Radial growth data have been used to detect early-warning signals of impending dieback, but they were not very successful in the case of oaks which show a high capacity to rapidly recover after drought (Cailleret et al., 2019). The variability in xylem vessel structure between years is a crucial factor in understanding the potential for adaptation in wood anatomy responses to drought (Argüelles-Marrón et al., 2023). Extensive meta-analyses examining the potential of xylem functional traits as indicators of tree vigor and decline in Mediterranean forests were presented by Borghetti et al. (2017, 2020). They evidenced that wood anatomical features serve as early warning signals of forest vulnerability in drought-prone regions. It is thus justified to search for differences in wood-anatomical traits between coexisting declining and non-declining trees which may subsequently be used as potential early-warning signals of tree mortality.

Hydraulic failure caused by climatic stress phenomena produce visible structural changes at the canopy level, such as desiccation and loss of vigor of the most marginal portions of the canopy (Nardini et al., 2013).

Overall, deciduous ring-porous oak species are regarded as drought-tolerant, anisohydric species which maintain high photosynthetic rates at low water potential (Epron and Dreyer, 1993; Roman et al., 2015). Additionally, they show the capacity to tap water from deep sources during dry periods (Skiadaresis et al., 2019; Ripullone et al., 2020; Kahmen et al., 2022). The large earlywood vessels of these species enable the maintenance of high hydraulic conductivity and stomatal conductance rates during the early growing season. (Klein, 2014; Guada et al., 2019). However, the formation of large vessels can also increase the vulnerability to drought by enhancing the risk of xylem embolism (Sperry et al., 1994; Pérez-de-Lis et al., 2018). In fact, deciduous oaks tend to form earlywood vessels with smaller lumen in drier sites (Alla and Camarero, 2012). Recent tree-ring studies indicate that the growth of deciduous oaks is vulnerable to drought, and the effects of previous drought events—referred to as legacies—vary depending on the species (Camarero et al., 2021; Bose et al., 2024). Drought legacies have also been found to affect also wood anatomy in the year following a drought event, resulting in the formation of smaller vessels (Süßel and Brüggemann, 2021), due to the importance of previous-year climate conditions on earlywood formation (Marchand et al., 2021). Thus, interannual variations in ring-width and vessel lumen dimensions offer complementary information on oak performance (Alla and Camarero, 2012; Colangelo et al., 2017a; Pérez-de-Lis et al., 2018; Guada et al., 2021), which might help to forecast dieback at tree level.

Moreover, not only do the size and density of vessels vary with environmental conditions, but drought can also alter the distribution of vessels within the rings, shifting from a ring-porous to a semi-ring porous structure, as observed in some *Fagaceae* species (Castagneri et al., 2020; Granda et al., 2017; Nola et al., 2020; Arnič et al., 2021). This means that the patterns of spatial aggregation and lumen size of vessels change within the earlywood. Favorable growth conditions during the previous winter can favor the formation of wide earlywood vessels (García-González and Eckstein, 2003; Marchand et al., 2021) even under subsequent dry conditions (Van der Werf et al., 2007). Warm temperatures and high moisture availability during the growing season enhance vessel enlargement and latewood formation (Gričar et al., 2013; Guada et al., 2021). However, the ring conductive area and latewood production decrease in response to drought (Alla and Camarero, 2012; Castagneri et al., 2020), and this might also be a consequence of the spatial arrangement of vessels and their variation in lumen size, which are proxies of phenotypic plasticity. Thus, year-to-year variations in vessel size, density, and overall conductive area can provide insights into climate limitations and potentially differentiate between declining and non-declining individuals (Fonti and García-González, 2008; Pérez-de-Lis et al., 2018). Additionally, given that vessel size varies within the ring, the potential of within-ring vessel size variation can be investigated as an early-warning signal of tree growth decline and forest dieback (Gričar et al., 2013).

We expect that drought will reduce the number and size of earlywood vessels thus affecting within-ring spatial clustering of vessels and their coefficient of variation in size. This is based on the importance of warm temperature and moisture availability for vessel formation and enlargement (Van der Werf et al., 2007; Gričar et al., 2013; Guada et al., 2021). Besides, we hypothesizes that spatial clustering of earlywood vessels will increase and variation in lumen size will decrease in trees exhibiting signs of drought-induced dieback, such as reduced growth rates.

This is fundamented on the importance that drought legacies can have on tree growth and ring formation (Süßel and Brüggemann, 2021). To test this hypothesis, we quantified and analysed year-to-year variations in radial growth and earlywood vessel area of five deciduous oak species showing different sensitivity to drought (*Quercus robur* L., *Quercus cerris* L., *Quercus frainetto* Ten., *Quercus canariensis* Willd., *Quercus humilis* Mill., *Quercus pubescens* Willd.) in forests across Spain and Italy. To assess potential differences between non-declining and declining trees, the study was carried out in sites showing evidence of drought-induced dieback and considered two vigor classes.

2. Material and methods

2.1. Study sites and tree species

We studied five deciduous, ring-porous oak species widely distributed in temperate and Mediterranean forests of Europe and showing recent drought-induced dieback. This was done in five sites located in Italy and Spain, where intensive monitoring of dieback phenomena was carried out (Table 1, **Fig. S1**). The selected species occupy wide biogeographical and climatic gradients from northern Europe to northern Africa and all are present and common in mixed forests of the Mediterranean Basin.

From a taxonomic perspective *Q. pubescens* in Italian and *Q. humilis* in Spanish sites are considered synonym of the same species (Di Pietro

et al., 2020). Indeed, *Q. pubescens* is considered a valid binomial across Europe, except for Spain, where it is replaced by *Q. humilis* Mill. (Amaral Franco, 1990). Given these regional differences in nomenclature and to maintain consistency with our previous studies, we have chosen to keep *Q. pubescens* (for Italian sites) and *Q. humilis* (for Spanish sites) separate in our analysis.

The Ticino site is a mixed floodplain forest spanning approximately 500 ha within the "Parco Lombardo della Valle del Ticino" in Northwest Italy near the Ticino river (Pericolo et al., 2023). The forest is primarily composed of pedunculate oak (*Quercus robur* L.), ash (*Fraxinus excelsior* L.), black alder (*Alnus glutinosa* (L.) Gaertn.) and elm (*Ulmus minor* Mill.). In this area, mean oak density and basal areas were 179 stems ha^{-1} and 18.8 m^2 ha^{-1}, respectively. Climate is temperate with a mean annual temperature of 12.8 °C and annual total precipitation of 1104 mm. Substrates are gravels and sand-clay deposits. According to local reports (DEPFAR, 2026), oaks showed decline symptoms since the early 2000s (shoot dieback, leaf loss and withering, epicormics shoots, growth decline and recent increase in mortality) (Colangelo et al., 2018a).

The Aramendia site is located in northern Spain. Here, uneven-aged stands of *Quercus humilis* Mill. were sampled. The study forest showed abundant dieback symptoms since 2017 affecting at least 25 % of the individuals, with scattered groups of recently dead trees (Camarero et al., 2021). This is a high forest with basic soils and understory dominated by *Buxus sempervirens* L., *Juniperus oxycedrus* L. and *Crataegus monogyna* Jacq. In this site, tree density and basal area were 1150 stems ha^{-1} and 36.9 m^2 ha^{-1}, respectively. Here, climate conditions are sub-Mediterranean and drier than in Ticino, with mean annual temperatures of 12.6 °C and annual precipitation of 620 mm. The two oak species studied in these mesic sites are shade-intolerant, with *Q. robur* dominant in valley bottoms with wet soils, and *Q. humilis* found in mountain sites with dry, basic soils across central and southern Europe (Damesin and Rambal, 1995).

In the Mediterranean Gorgoglione site, located in the mountainous Basilicata region (southern Italy), *Q. pubescens* Willd. and *Quercus cerris* L. mixed stands was sampled. This is a high forest with a mean density of 600 stems ha^{-1} dominated by *Q. cerris* (71 % of basal area) followed by *Q. pubescens* (25 % of basal area) and other broadleaf species. *Q. pubescens* occupies the most xeric sites (e.g., low-elevation sites steep slopes with southern aspect and shallow soils), whilst *Q. cerris* abounds in more mesic locations. Soils are a mixture of sand, silt and clay textures (Colangelo et al., 2018b). Climate conditions correspond to cool-wet winters and dry-warm summers with mean annual temperature of 11.6 °C and annual precipitation of 722 mm. The two oak species showed decline symptoms since 2007 with the most affected area spreading across ca. 450 ha and including many trees with defoliation >50 % and patches with 15 % of dead trees (Ripullone et al., 2020). Soils are sandy-loam textured with a mean pH of 7.5 and shallow.

The second Mediterranean Italian site is located near San Paolo Albanese in the Basilicata region, where we sampled a pure high forest of *Quercus frainetto* Ten. This stand has a density of 348 stems ha^{-1} (Colangelo et al., 2017a). *Q. frainetto* is a light-demanding oak species sensitive to dry conditions in late spring and summer, but thrives in mesic sites with deep soils (Gentilesca et al., 2017). The climate is characterized by warm, dry summers, with a mean annual temperature of 16.4 °C and annual precipitation of 742 mm. The area features sandy soils, and these stands were traditionally managed as coppices with livestock grazing. Dieback symptoms started in the early 2000s and corresponded to abundant leaf loss and withering, growth decline and high mortality (Colangelo et al., 2017a, 2017b, Colangelo et al., 2018a, 2018b). In affected stands, 10–15 % of trees recently died.

The Gamir site is located within "Los Alcornocales" Natural Park, Andalusia (southwestern Spain). Here, *Quercus canariensis* Willd. trees were sampled in stands with mean density of 54 stems ha^{-1} (Sánchez-Salguero et al., 2020). This Mediterranean oak inhabits sites with acid soils in humid and warm areas of southern Spain and northwestern Africa, where its growth is constrained by dry and warm spring-summer conditions (Gea-Izquierdo et al., 2012). Climate in the study area is Mediterranean with wet and mild winters and dry and warm summers, corresponding to a mean annual temperature of 16.4 °C and annual precipitation of 560 mm. Intense dieback was observed here following the severe drought of 2005. Additionally, the invasive oomycete *Phytophthora cinnamomi* Rands. is widespread in the area and has contributed to oak decline, particularly in poorly drained sites with high soil moisture retention (Serrano et al., 2022).

2.2. Field sampling

In study sites, a pairs of dominant and neighboring oak trees with contrasting vigor non-declining (ND) and declining (D) couples were selected to estimate their growth trends using dendrochronology. Within each ND–D couple, trees were 10–15 m apart at maximum. First, five to seven circular plots (radius of 15 m) were randomly located in each site to characterize the stand structure (density, basal area). Second, in each plot, the vigor of each mature oak individual was characterized by a visual assessment of crown defoliation (Dobbertin, 2005). Oaks were classified into two vigor categories based on crown transparency: declining trees (D) had crown transparency exceeding 50 %, while non-declining trees (ND) had transparency below 50 %. We measured the diameter at breast height (dbh) of sampled oaks at 1.3 m using measuring tapes and measured tree height using a Nikon TruPulse 360 laser rangefinder. Pairs of neighboring oak trees with contrasting vigor (ND–D couples) were selected at each study sites to compare their growth and wood anatomy series.

2.3. Climate data and drought index

To characterize the climatic conditions of study sites, monthly maximum and minimum temperatures and precipitation data were obtained from the 0.25°-gridded *E*-OBS database (https://climexp.knmi.nl/start.cgi) for the period 1950–2018 (Cornes et al., 2018). We used this data set to avoid problems in homogeneity or gaps in local series, which usually do not cover periods longer than 30 years. In addition, the Standardized Precipitation–Evapotranspiration Index (SPEI) was used to assess the severity and duration of droughts. The SPEI is a multiscalar drought index that accounts for both precipitation and evapotranspiration, calculated over various time scales (Vicente-Serrano et al., 2010). Positive and negative SPEI values indicate wet and dry conditions, respectively. Monthly SPEI data were downloaded for time scale of 12 months and at a 0.5° spatial resolution using the SPEI Global Drought Monitor webpage https://spei.csic.es/map/maps.html (https://spei.cs

Table 1
Characteristics of the study sites. The ratio between annual precipitation and evapotranspiration (P / PET, last column) was obtained from Zomer et al. (2022).

Site	Species	Latitude (N)	Longitude (−W, +E)	Elevation (m a.s.l.)	Slope (%)	Aspect	Year of dieback onset	P / PET
Ticino	*Q. robur*	45.436	8.825	115	0	–	2004	4.9
Aramendia	*Q. humilis*	42.716	−2.112	683	9	SE	2017	2.2
Gorgoglione	*Q. cerris*	40.368	16.174	850	25	E	2007	1.8
Gorgoglione	*Q. pubescens*	40.368	16.174	800	30	E	2007	1.8
San Paolo A.	*Q. frainetto*	40.020	16.341	970	25	SO	2003	1.4
Gamir	*Q. canariensis*	36.570	−5.534	510	15	SE	2005	1.1

ic.es/map/maps.html).

2.4. Tree-ring width series

For each species, we selected 12–34 paired trees of different vigor, i.e., neighboring ND and D oaks located 10–15 m apart at maximum (Table 2). They were sampled in late summer of 2017 to quantify their radial-growth trends using dendrochronology (Fritts, 1976). Two cores were sampled at 1.3 m from each tree at opposite directions and perpendicular to the maximum slope using a 5-mm Pressler increment borer. The transversal surface of cores was cut using a sledge microtome to differentiate the annual rings (Gärtner and Nievergelt, 2010). Rings were visually cross-dated and measured with precision of 0.01 mm using a binocular microscope coupled to a computer with the LINTAB package (Rinntech, Heidelberg, Germany). The COFECHA program was used to evaluate the statistical cross-dating of tree-ring width data (Holmes, 1983). To quantify growth trends and to remove part of age and size-related decrease in tree-ring width, we transformed these data into annual basal area increment (BAI) assuming a circular shape of stems and using the formula:

$$BAI = \pi \left({r_t}^2 - {r_{t-1}}^2 \right) \quad (1)$$

where r_t and r_{t-1} represent the width of the rings in the year t and t-1, respectively. Mean BAI series were calculated by averaging the BAI series of the individuals of each vigor class sampled in each site. Tree age at 1.3 m was estimated from increment cores that either included the pith or were close to it, i.e. the innermost rings were clearly curved.

2.5. Earlywood anatomy

For each vigor class (ND and D trees), we selected five trees per site and one radius per tree to perform the analyses of earlywood anatomy. Selected trees were those showing the highest correlation between their BAI series and the mean site BAI series. Wood anatomy was analysed for the common period from 1980 to 2017. First, wood cross-sections were obtained using a sledge microtome (Gärtner and Nievergelt, 2010). Cores from each tree were subdivided into pieces approximately 2–5 cm long. Thin sections (thickness of 10–20 μm) were then cut from each piece with the microtome, stained with safranin (1 %) and Astra blue (2 %), and fixed with Eukitt®. Second, high-resolution images of the sections were captured using an Olympus BH2 microscope equipped with an Olympus DP73 camera. The images were stitched with the PT-Gui software (New House Internet Services BV, Rotterdam, NL) to create one composite image for each sample. The images were analysed using the image analysis freeware ImageJ ver. 1.54i (Schneider et al., 2012). This allowed measuring the area and the radial diameter (d), assuming a circular shape, and centroid position of each earlywood vessel within each ring. The lower limit for vessel identification was set at a diameter of 50 μm. The vessels were measured in a tangential window of 2 mm.

Then, we calculated for each ring the earlywood vessel density (Scholz et al., 2013). The earlywood hydraulic diameter (*Dh*) was calculated as the average of $\sum d^5/\sum d^4$ (Sperry et al., 1994). The *Dh* was calculated considering all measured earlywood vessels and used to calculate mean series for each vigor class and site. In addition, the position of each vessel within the ring (x and y coordinates) was recorded.

Using the individual vessel area data, we estimated the average size of vessel in 10 equally spaced portions of the earlywood within each ring. We have divided the coordinates of the vessels by 10 sections in order that the centroid of each vessel could only be included in one section. That is, we divided the earlywood in 10 radial sections from the bark to the pith and estimated the average size of vessels and the number of vessels in each section. Doing so, each ring was represented by 10 portions irrespectively of their size. In addition, we obtained the coefficient of variation of vessel area (hereafter CV) and a spatial aggregation index (hereafter AI) (Clark and Evans, 1954). The AI is a measure of clustering calculated as the ratio between the observed distance to the nearest neighbor and that expected distance under a Poisson process equivalent to complete spatial randomness. An AI value >1 indicates that objects are regularly distributed, while a value <1 indicates clustering. We used the AI to weight the CV by calculating their product. Thus, high values of CV × AI show the presence of regularly spaced earlywood vessels which vary in area, while lower values of CV × AI indicate a clustered distribution of vessels with similar area.

2.6. Statistical analyses

We conducted a series of statistical analyses to compare tree characteristics and model earlywood vessel patterns. The non-paramtric Mann-Whitney *U* test was used to compare dbh, height, age, BAI, *Dh*, vessel area, and density between declining (D) and non-declining (ND) trees within each site since some variables (dbh, age) did not follow normal distribution according to Shapiro-Wilk tests.

Generalized additive mixed effect models (GAMMs; Wood, 2017) were employed to analyze how vessel area and number varied within the earlywood ring and between vigor classes. The earlywood was divided into 10 radial sections from the bark to the pith with distance class (1−10), vigor class, and their interaction as explanatory variables. Each ring was represented by 10 portions irrespectively of their size. in order to observe the variation in the area and number of vessels in relation to the distance from the innermost part of the earlywood (annular section 1) to the outermost part (annular section 10). Tree identity and year were included as random factors to account for repeated measures. Linear mixed-effects models (LMMs; Pinheiro and Bates, 2000) were used to test if vessel size and number progression differed between D and ND trees in relation to the drought index (SPEI). LMMs were used to test for differences in BAI and earlywood anatomical characteristics (vessel area and density, *Dh,* AI, CV, and CV × AI) between vigor classes from

Table 2
Characteristics of the sampled ND and D oak trees. Values are presented as means ± standard error (SE). The basal area increment (BAI) data correspond to the period 1980–2017. Different letters indicate significant differences ($p < 0.05$; Mann-Whitney *U* tests) between tree types within each site.

Site	Species	Vigor class	No. trees	Dbh (cm)	Height (m)	Age at 1.3 m (yrs.)	BAI ($mm^2\ yr^{-1}$)	*Dh* (μm)	Vessel density (No. mm^{-2})
Ticino	*Q. robur*	ND	27	52.4 ± 2.4b	25.1 ± 0.9b	79 ± 3	2199 ± 77b	373 ± 3.8b	58 ± 2a
		D	19	38.7 ± 1.8a	15.3 ± 0.6a	84 ± 3	983 ± 47a	332 ± 3.5a	62 ± 2a
Aramendia	*Q. humilis*	ND	17	27.1 ± 1.3a	11.4 ± 0.2b	69 ± 9	416 ± 14b	297 ± 3.3a	66 ± 3a
		D	15	21.7 ± 1.1a	9.2 ± 0.4a	74 ± 10	183 ± 8a	287 ± 2.9a	62 ± 2a
Gorgoglione	*Q. cerris*	ND	23	32.0 ± 0.8b	15.0 ± 0.4b	102 ± 4	539 ± 36b	317 ± 3.7a	16 ± 1a
		D	22	28.0 ± 0.7a	12.2 ± 0.4a	107 ± 2	343 ± 18a	298 ± 3.7a	14 ± 1a
	Q. pubescens	ND	25	26.6 ± 1.0b	11.5 ± 0.3b	115 ± 4	318 ± 19b	289 ± 2.0a	71 ± 3a
		D	19	22.2 ± 0.7a	8.6 ± 0.3a	110 ± 3	195 ± 8a	274 ± 2.5a	69 ± 4a
S. Paolo	*Q. frainetto*	ND	34	33.3 ± 0.7a	13.5 ± 0.5b	140 ± 7	396 ± 16b	323 ± 2.7a	59 ± 2b
		D	34	31.9 ± 0.9a	10.2 ± 0.4a	132 ± 5	307 ± 11a	316 ± 3.5a	40 ± 1a
Gamir	*Q. canariensis*	ND	12	51.3 ± 2.1a	11.7 ± 0.2a	107 ± 4	1115 ± 35b	281 ± 3.5b	41 ± 1a
		D	12	52.3 ± 4.3a	11.1 ± 0.5a	112 ± 5	936 ± 38a	221 ± 3.5a	44 ± 2a

1980 to 2017. BAI was modeled against vigor class, calendar year, and their interaction, with tree identity as a random variable. To test for generality across species, we included all species in the model with tree ID nested within species as a random factor.

GAMMs were used to model the response of *Dh* and CV × AI to drought severity (SPEI) and vigor class. Individual log-transformed BAI, AI, and CV × AI were adjusted as a function of calendar year using thin-plate regression splines (maximum 3 degrees of freedom; Wood, 2003). Interactions between calendar year and vigor class were considered to account for divergences between ND and D trees. Tree identity nested within species was included as a random effect, and a first-order autocorrelation structure was applied to account for BAI dependency between consecutive years.

All analyses were performed using R (R Core Team, 2024), with LMMs and GAMMs fitted using the *nlme* (Pinheiro et al., 2023) and *mgcv* (Wood, 2011) packages, respectively.

3. Results

3.1. Trees features and growth patterns

Declining (D) trees exhibited smaller diameters compared to non-declining (ND) trees, with the exception *Q. cerris* and *Q. pubescens* in Gorgoglione, as well as *Q. frainetto* in S. Paolo A. (Table 2). In most sites, ND trees were taller than D trees, except for *Q. canariensis* in Gamir. Although no significant differences in age were observed between ND and D trees (**Table S4**), the mean basal area increment (BAI) values were consistently higher for ND trees than for D trees, where the ND trees grew from 20 % to over 50 % more than the D (Fig. 1**, Fig. S3**). Early-wood anatomical variables showed contrasting results depending on the

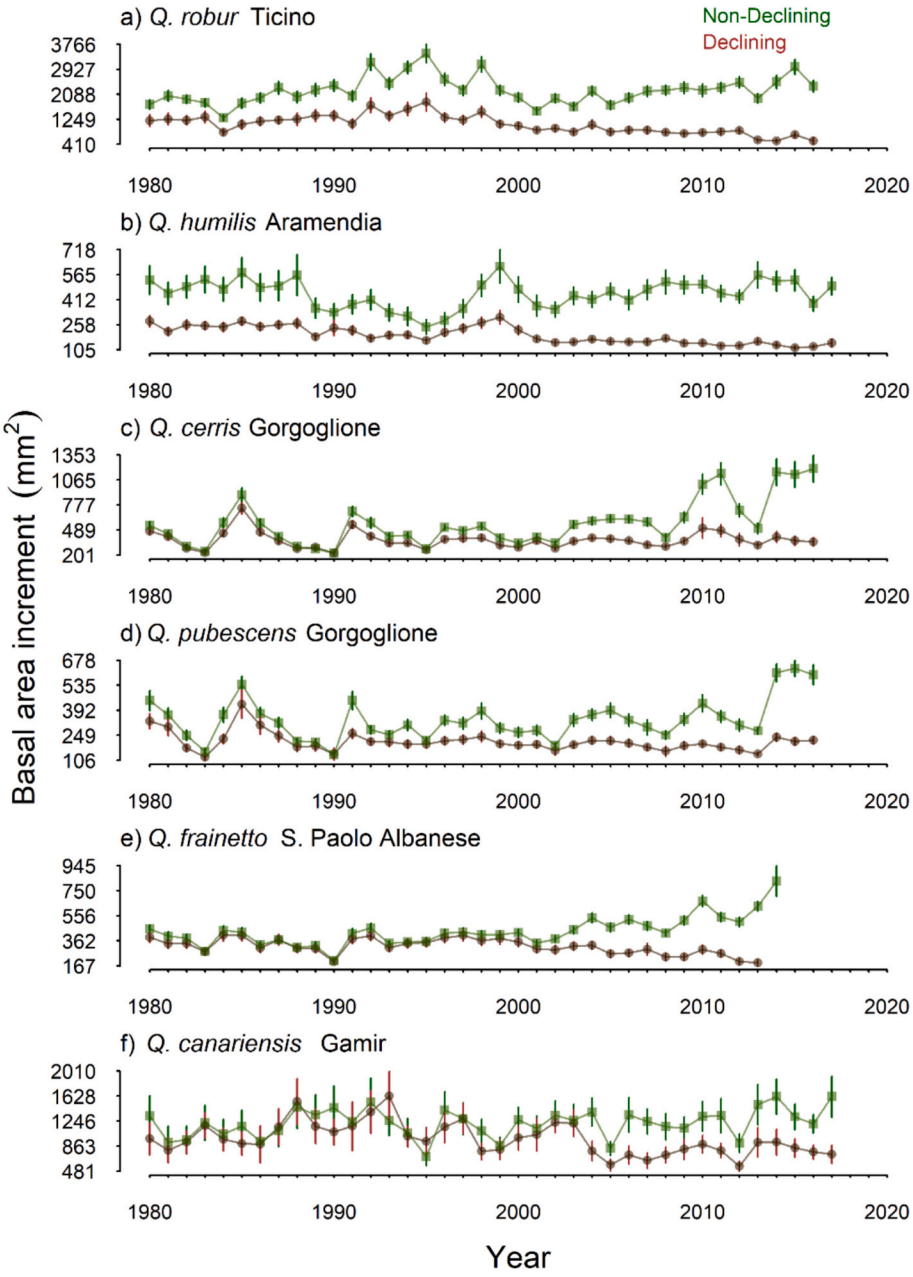

Fig. 1. Variation in basal area increment between non-declining trees (represented by dark green lines and squares symbols) and declining trees (represented by brown lines and points symbols) for each species at the study sites. The points and lines indicate mean values across individuals, while the vertical segments represent the standard errors of the mean.

species with *Dh* being higher in ND than in D trees of *Q. robur* and *Q. canariensis*, and vessel density being higher in ND *Q. frainetto* individuals.

We observed significant differences in BAI and its trend between ND and D trees in each species (**Table S1;** Fig. 2). However, the divergence in BAI between vigor classes prior to dieback onset differed in duration and magnitude among species and sites. Specifically, the divergence was greater (values between 1249 and 3000 mm^2) and persisted longer in *Q. robur* compared to the other species (Fig. 1). The strongest BAI difference between ND and D trees observed during the last years corresponded to *Q. cerris* and *Q. frainetto*.

3.2. Variations in earlywood vessel area and density

A variation in the area and number of vessels was observed in relation to the distance from the innermost part of the earlywood (annular section 1) to the outermost part (annular section 10) (Fig. 2). For all species, the vessel area decreased from the pith to the bark, as expected. Overall, the vessel area in the first portion of the earlywood was larger in ND trees than in D trees. This was particularly evident in *Q. pubescens* from Gorgoglione and less evident in *Q. frainetto*. The number of vessels tended to increase from the middle (section 4) towards the end of the earlywood in most cases, with the exception of *Q. cerris* in Gorgoglione. ND trees showed more vessels in the last formed half of the earlywood, which were often of lower area than in D trees (Fig. 2). Overall, the SPEI exerted little significant influences on the change in vessel area along the earlywood and this effect depended on the species (Table 3). A significant interaction between earlywood section and SPEI was found in *Q. humilis*, *Q. cerris* and *Q. pubescens* but only in declining trees (Table 3).

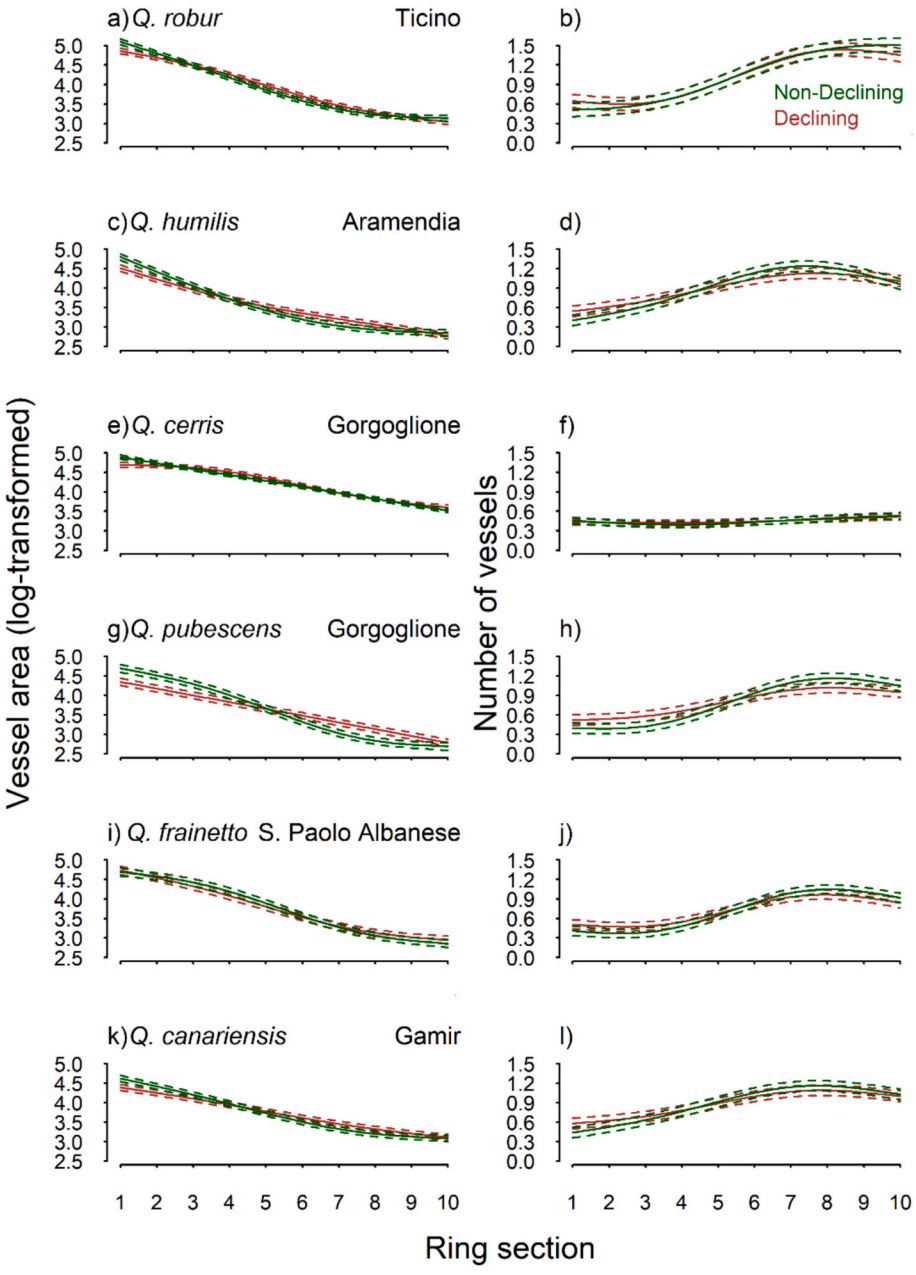

Fig. 2. The variation in vessel area (μm^2), on the left, and number, on the right, as a function of the distance from the innermost part of the earlywood (ring section 1) to the outermost part (ring section 10). Non-declining are represented by green lines, while declining trees are indicated by red lines.

Table 3
Trends in vessel area assessed within the earlywood 10 sections (with distance class 1–10) compared between D and ND vigor classes as a function of drought severity (SPEI). The *F* statistics associated with the variables are shown. Significant values (p. < 0.05) are indicated with*.

Site	Species	Declining trees			Non-Declining trees		
		Section	SPEI	Section × SPEI	Section	SPEI	Section × SPEI
Ticino	*Q. robur*	4048.06*	2.60	4.36*	5429.53*	0.47	1.60
Aramendia	*Q. humilis*	1770.89*	8.81*	13.52*	3721.24*	6.17*	3.41
Gorgoglione	*Q. cerris*	964.23*	5.65*	9.022*	2395.39*	1.67	0.67
	Q. pubescens	1078.93*	2.79	9.38*	4040.87*	0.85	0.01
S. Paolo	*Q. frainetto*	1778.41*	0.33	0.06	2386.80*	1.74	1.40
Gamir	*Q. canariensis*	2269.42*	1.46	0.40	4177.85*	0.24	0.63

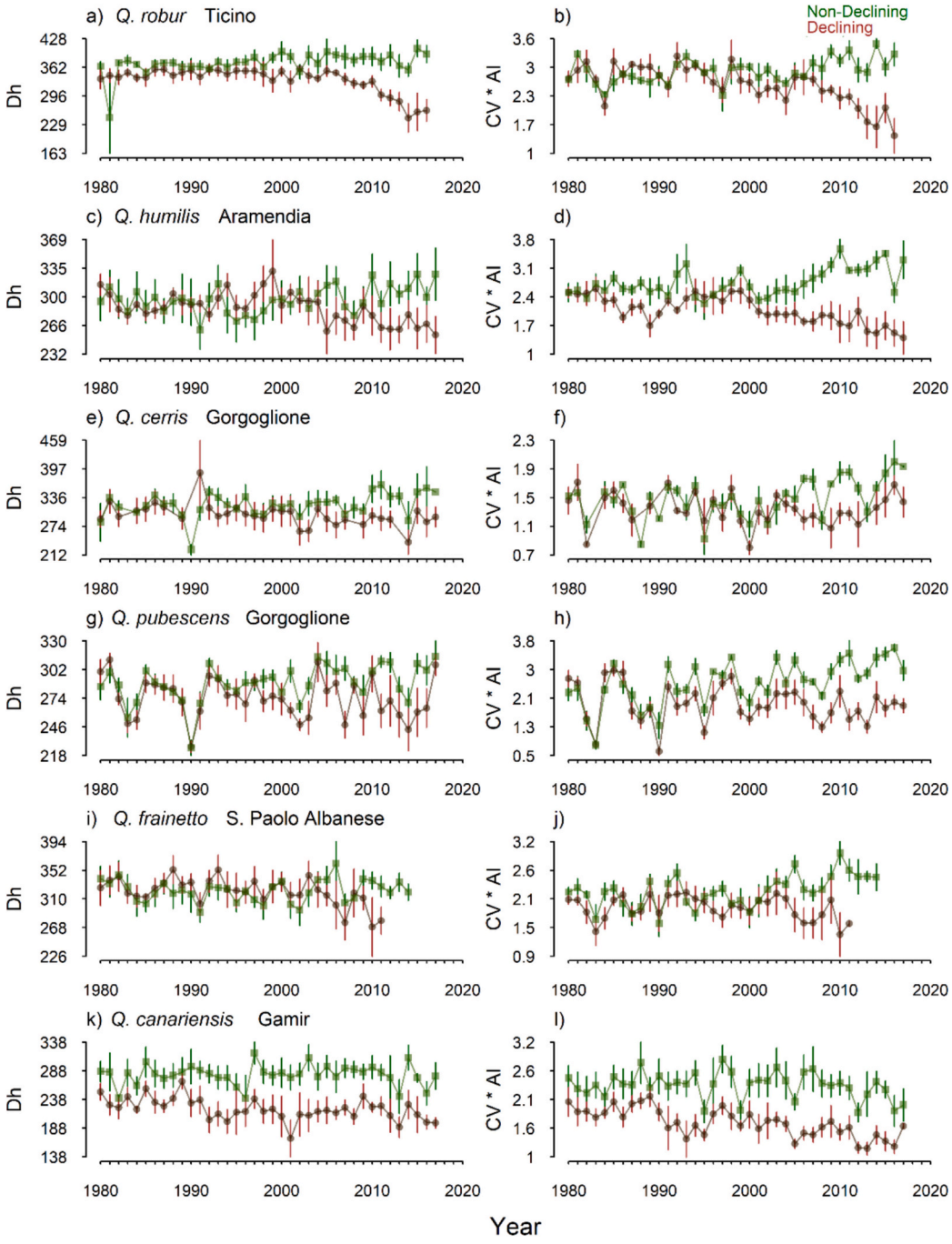

Fig. 3. Variation in hydraulic diameter (*Dh*, in μm), on the left, and the product (CV × AI) of its coefficient of variation (CV) and aggregation index (AI), on the right, for non-declining trees (represented by green lines and squares symbols) and declining trees (represented by brown lines and points symbols). Solid lines indicate the estimated relationships, while dashed lines represent the 95 % confidence intervals (CIs) of these estimates.

3.3. Changes in hydraulic diameter and its spatial variability

Differences in *Dh* through time between ND and D trees were apparent in some species and sites, particularly in the cases of *Q. robur* and *Q. canariensis* with wider vessels in ND trees (Fig. 3 **Table S2**). The D trees showed a long decline of CV several decades prior to dieback in all sites, where the ND showed differences up to double the values compared to D, being particularly strong in *Q. robur*, *Q. humilis*, *Q. pubescens* and *Q. canariensis*, but not in the case of *Q. cerris* (**Fig. S2**).

Conversely, the AI showed divergences between ND and D trees only in *Q. humilis* and *Q. pubescens* with higher values in ND trees. Finally, the CV × AI showed higher values in ND trees of all sites, although they were lower in *Q. cerris* (Fig. 3 **Table S3**). In this case the divergence between ND and D trees was pronounced in *Q. robur* and *Q. humilis*, with differences in the values between the two categories ranging from 0.5 to of 2.0 (Fig. 3).

3.4. Relationships between the drought index and the vessel hydraulic diameter

The relationship between the SPEI and the *Dh* and CV × AI varied between sites and oak species (Table 4). In general, the *Dh* was less related with the SPEI than CV × AI, particularly in the case of *Q. canariensis*, and also *Q. cerris* and *Q. pubescens* from Gorgoglione. The CV × AI allowed separating ND and D trees in most sites and species, excepting *Q. cerris* and *Q. frainetto*. These results indicated different responses of earlywood anatomy to drought in ND and D trees.

We observed distinct responses of hydraulic diameter (*Dh*) and the product of coefficient of variation and aggregation index (CV × AI) to drought severity (SPEI) between ND and D trees (Table 4). The relationship between *Dh* and SPEI was not significant for both vigor classes (Table 4) as well as when all species were considered in the same model (Fig. 4). However, the association between SPEI and CV × AI differed between ND and D trees. While D trees exhibited a linear relationship, ND trees showed a non-linear response with a saturation effect. This suggests that ND trees can complete earlywood formation in spring under more mesic conditions (lower SPEI values) compared to D trees.

3.5. Relationships between growth (BAI), the vessel hydraulic diameter and CV × AI

Overall, we found a positive relationship between BAI and Dh and CV × AI for (**Fig. S4, Tables S5, S6**), but with differences in their magnitude between sites and vigor classes. The greatest differences between ND and D trees were observed in *Q. humilis* and *Q. canariensis* but with opposite patterns since ND trees were more strongly linked in *Q. humilis* while in *Q. canariensis* the relationship was stronger for D trees. Observing the relationships between BAI and CV × AI, differences between vigor classes emerged in the wettest (*Q. robur*) and driest (*Q. pubescens*) sites. Lastly, regarding the associations between Dh and CV × AI, we observed positive linear relationships between these two variables in the two vigor classes, with few differences between ND and D excluding the case of *Q. robur* in Ticino (**Fig. S5, Tables S7**).

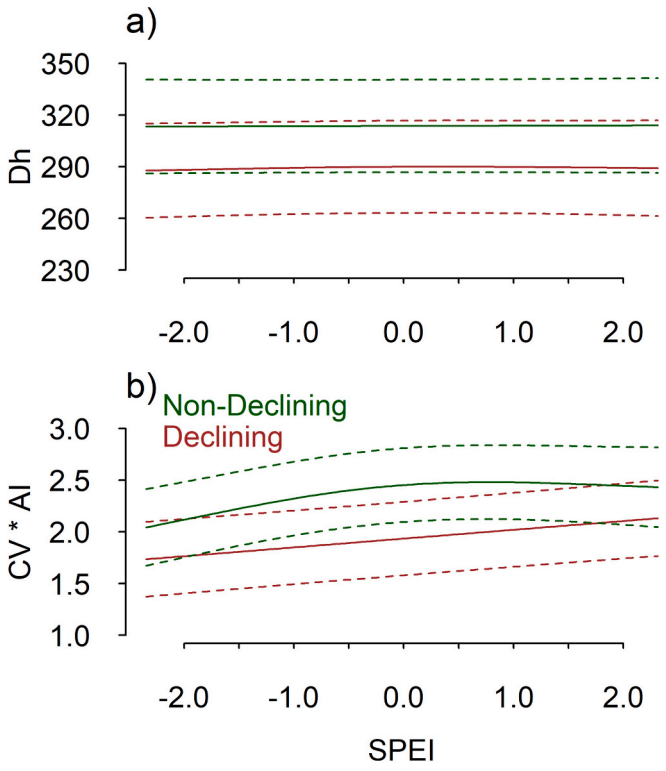

Fig. 4. Relationship between the drought index (12-month SPEI) and earlywood hydraulic diameter (Dh) (a); product of vessel size coefficient of variation (CV) and spatial aggregation index (AI) (CV × AI, b), in non-declining (green lines) and declining (red lines) trees across species. Solid lines represent estimated relationships, while dashed lines indicate 95 % confidence intervals.

4. Discussion

We show that the spatial configuration of earlywood vessels allows differentiating between declining and non-declining trees in deciduous ring-porous oaks. Notably, measures of dispersion (CV) and spatial aggregation (AI) of earlywood vessel area effectively separated individuals according to their vigor in most studied oak species. This finding confirms our hypothesis that within-ring variation in vessel lumen area is a crucial factor when comparing the responses of declining and non-declining trees to drought stress and can serve as an early-warning

Table 4
Relationship between the hydraulic diameter (*Dh*) and the product between the coefficient of variation in vessel size and the aggregation index (CV × AI) with the 12-month drought index (SPEI 12) for declining (D) and non-declining (ND) trees. For each species in each site, the *F* statistic associated with the vigor class and the degrees of freedom associated with the spline (GAM) terms are shown. Significant values are indicated with * ($p < 0.05$) and ** ($p < 0.01$).

Site	Species	Variable	Vigor	D × SPEI 12		ND × SPEI 12		
Ticino	*Q. robur*	Dh	36.37 ± 17.40*	1	0.57	1	0.77	0.14
		CV × AI	0.29 ± 0.14*	1.76	1.77	1	0.98	0.04
Aramendia	*Q. humilis*	Dh	10.82 ± 19.68	1	3.02	1.61	3.46	0.01
		CV × AI	0.693 ± 0.21**	1.70	1.93	1.00	0.46	0.22
Gorgoglione	*Q. cerris*	Dh	21.64 ± 23.21	1.67	1.23	1.86	2.73	0.05
		CV × AI	0.14 ± 0.07	1.00	6.76**	1.70	9.43**	0.09
	Q. pubescens	Dh	17.72 ± 10.74	1	0.01	1.41	2.00	0.07
		CV × AI	0.64 ± 0.18**	1	23.20**	1.90	22.15**	0.25
S. Paolo	*Q. frainetto*	Dh	−0.64 ± 18.57	1	0.57	1	4.46*	<0.01
		CV × AI	0.33 ± 0.20	1	0.03	1	2.70	0.08
Gamir	*Q. canariensis*	Dh	60.22 ± 20.90**	1	0.09	1	0.07	0.27
		CV × AI	0.70 ± 0.21**	1.70	5.86*	1.80	20.1**	0.32

signal of oak decline. Below we discuss how these anatomical features can be viewed as responses to dry conditions improving vessel connectivity and hydraulic conductivity.

Deciduous, ring-porous oaks adopt an anisohydric strategy (Hochberg et al., 2018). This strategy depends on their ability to rapidly conduct water in the early growing season, to access deep water sources and to store carbohydrates in their xylem rays, contributing to their high recovery after drought (Ripullone et al., 2020; Zhang et al., 2024). Consequently, oaks exhibit shorter and less pronounced post-drought legacy effects compared to coexisting tree species (Anderegg et al., 2015; Gazol et al., 2020; Bose et al., 2024). This resilience makes forecasting oak decline and dieback using tree-ring series depending on species-specific and contingent on site conditions (Cailleret et al., 2019). Wood anatomy may offer a more robust tool for detecting trees experiencing a progressive loss of vigor induced by water shortage, i.e., declining trees prone to mortality.

The observed differences in earlywood anatomy between declining and non-declining trees can be attributed to several underlying mechanisms. For instance, trees subjected to chronic water shortage may alter their xylem structure to improve hydraulic safety, a process known as hydraulic adjustment (Fonti et al., 2010). This adjustment can lead to the formation of smaller vessels or changes in vessel distribution within the earlywood. Additionally, drought stress can alter carbon allocation patterns, potentially reducing resources available for earlywood vessel formation (McDowell et al., 2011). These shifts in carbon allocation may result in fewer or smaller vessels being formed during periods of water stress. Phenological changes induced by water stress may also play a role in the observed anatomical differences. Drought can affect the timing and duration of earlywood formation, which in turn can result in changes to vessel characteristics before overall growth is impacted (Sass-Klaassen et al., 2011). This suggests that earlywood anatomy may be a more sensitive indicator of drought stress than growth metrics. Furthermore, legacy effects of drought on cambial activity and stored carbohydrates may influence earlywood formation in subsequent years, resulting in the accumulation of anatomical changes over time (Anderegg et al., 2015).

Trees of different vigor or defoliation classes exhibited contrasting values of CV × AI, except in *Q. cerris* and *Q. frainetto*, which showed recent divergences in this variable between non-declining (ND) and declining (D) trees from the 2000s onwards. In other cases, ND and D trees displayed different CV × AI values between 10 and 30 years before the onset of decline/dieback. Generally, growth (BAI) divergences between ND and D trees were longer-lasting (at least 30–40 years) in the wettest sites (*Q. robur* in Ticino, *Q. humilis* in Aramendia). Growth divergence between ND and D trees increases when growth begins to decline in response to severe drought conditions. Furthermore, regarding these divergences, in the wettest sites the metrics CV × AI were more pronounced. This differential behavior suggests that CV × AI is a more effective and functional measure of the recent loss of vigor than tree-ring width. In both cases, the responses corresponded to warm-dry stress conditions linked to droughts occurring in the early 21st century (Colangelo et al., 2017a, 2018a; Gentilesca et al., 2017; Camarero et al., 2021).

The stronger differentiation observed in more mesic sites (e.g., *Q. robur* in Ticino, *Q. humilis* in Aramendia) compared to drier sites suggests that trees growing under chronic water deficit may have less capacity for anatomical adjustment. This observation aligns with the concept that trees in more favorable environments may have a greater range of anatomical responses to drought stress, while those in chronically dry conditions may already be operating near their physiological limits (Bréda et al., 2006; Bose et al., 2024).

Earlywood vessel area reflects changes in theoretical hydraulic conductivity and tree vigor, linked to decreases in hydraulic diameter (*Dh*) and growth rates after drought (Corcuera et al., 2004). Generally, declining trees exhibit lower growth rates and smaller earlywood vessel lumens than non-declining trees (Camarero et al., 2015; Colangelo et al., 2017a; Cailleret et al., 2019). However, this pattern is not universal; in some instances, fast-growing, water-spending trees forming wide vessels may be more vulnerable to drought due to being hydraulically underbuilt for tolerating water shortage, as observed in *Q. robur* (Levanič et al., 2011) and discussed in Borghetti et al. (2020). This scenario does not appear to apply to our study sites, where vigorous trees tended to form wider vessels.

Discrepancies between studies may also arise from changes in vessel diameter within the earlywood related to cambial phenology, as illustrated by *Q. pubescens* from Gorgoglione site. Here, the ND trees formed wider vessels in the early earlywood, corresponding to the spring period when soil water content, photosynthetic rates and growth rates typically peak in deciduous trees (Michelot et al., 2012). These trees then produced smaller vessels in the late earlywood, which are less prone to embolism, compared to declining trees.

We also acknowledge that due to the practical constraints of our sampling methodology, it was not feasible to select declining (D) and non-declining (ND) trees of identical size across all study sites. Consequently, we cannot entirely rule out the potential influence of ontogenetic effects on vessel size, as highlighted by Olson et al. (2014) in their large-scale investigation of angiosperm species.

The lack of differentiation capacity of CV × AI in cases such as *Q. cerris* could be explained by the subjective classification of trees into two vigor classes, which may change over time in sites subjected to chronic drought stress. The non-linear and linear responses of CV × AI to the drought index in non-declining and declining trees, respectively, suggest different timings and rates of earlywood formation and tree-ring growth between these groups.

A more comprehensive understanding of vessel lumen variations within growth rings can be achieved by linking these changes to fluctuations in growth rate and water-use efficiency. A promising approach could combine intra-annual growth monitoring through xylogenesis or dendrometers with the use of isotopic proxies ($\delta^{13}C$, $\delta^{18}O$) to track water and gas exchange. Integrating these methods can provide deeper insights into the physiological mechanisms underlying the adjustment of vascular structure in response to environmental changes. This approach may reveal crucial information about the resilience to drought of oak species.

The measurement of vessel clustering is based on the notion that once a xylem vessel becomes embolized, vessel connections can provide pathway continuity (Carlquist, 1977). Two- to three-dimension analyses of xylem vessel distribution have received attention in wood anatomy studies and measures such as vessel grouping, aggregation, and connectivity have been carried out (Scholz et al., 2013). In this sense, a simple vessel grouping index was developed by Carlquist (2001), corresponding to the total number of vessels divided by the total number of vessel groupings. However, that index did not take into account the diameter of vessels. Alternative grouping indices based on vessel connectivity in transverse sections and point pattern analyses were developed by Mencuccini et al. (2010) and Martínez-Vilalta et al. (2012), who focused on conduit density-packing relationships. Here we go a step further by investigating how variations in vessel clustering vary between years and considering tree vitality. As a measure of clustering, we opted to use the Clark Evans index (Clark and Evans, 1954) that does not account for the variations in vessel size. However, we weighted the aggregation index with the coefficient of variation accounting for within tree-ring earlywood vessel size differences that can arise due to climate constraints (García-González and Eckstein, 2003; Van der Werf et al., 2007; Gričar et al., 2013; Castagneri et al., 2020; Guada et al., 2021; Marchand et al., 2021; Süßel and Brüggemann, 2021). In line with our hypothesis, variations in the proposed index suggest that spatial clustering of earlywood vessels increase while variation in lumen size decreases in oaks exhibiting signs of drought-induced dieback. This synthetic measure offers information on year-to-year variations in earlywood vessel clustering and size asymmetry, a metric that can complement existing measures of tree ring width and hydraulic

conductivity enhancing our capacity to detect early warning signals of tree decline.

5. Conclusions

Our research establishes earlywood vessel characteristics as valuable early-warning signals of oak decline, offering a promising tool for proactive forest management in the face of increasing climate-related drought stress. Changes in earlywood vessel area dispersion (CV) and spatial arrangement (AI) represent significant yet understudied indicators of dieback and growth decline in oak species. We provide evidence that the product of these two variables (CV × AI) differentiates trees based on their vigor and response to drought stress in temperate and Mediterranean oak forests.

The CV × AI metric detected divergences between non-declining and declining trees as early as 10 to 30 years before the onset of visible dieback symptoms appeared, outperforming radial-growth measures, such as basal area increment (BAI), in most cases. This suggests that changes in earlywood vessel anatomy may precede and be more sensitive to incipient drought stress than radial growth. The non-linear response of CV × AI to drought severity in non-declining trees, compared to the linear response in declining trees, further underscores the complex physiological adjustments reflected in wood anatomy.

Our findings have implications for forest management and monitoring under climate change. The ability to identify vulnerable trees before visible crown symptoms appear could enable more timely and effective interventions. Additionally, the long-term nature of anatomical records allows for retrospective analyses of forest responses to past climate extremes, thereby informing future management strategies.

In perspective, the proposed methodology and the evidence that emerged in this work can provide an approach to be used in predictive and interpretative models in order to characterize the phenomenon of Mediterranean oak decline.

CRediT authorship contribution statement

Michele Colangelo: Writing – original draft, Visualization, Validation, Supervision, Software, Methodology, Investigation, Data curation, Conceptualization. **Antonio Gazol:** Writing – original draft, Visualization, Validation, Supervision, Software, Methodology, Investigation, Formal analysis, Data curation, Conceptualization. **J. Julio Camarero:** Writing – original draft, Visualization, Supervision, Software, Methodology, Investigation, Data curation, Conceptualization. **Marco Borghetti:** Writing – review & editing, Supervision. **Raúl Sánchez-Salguero:** Writing – review & editing. **Luis Matias:** Writing – review & editing. **Maria Castellaneta:** Writing – review & editing. **Paola Nola:** Writing – review & editing. **Francesco Ripullone:** Writing – review & editing, Supervision, Methodology, Conceptualization.

Funding

This study was carried out within the Agritech National Research Center and partially financed by the European Union Next-Generation funds (Piano Nazionale di Ripresa e Resilienza (PNRR) – Missione 4 Componente 2, Investimento 1.4 – D.D. 1032 17/06/2022, CN00000022) This manuscript reflects only the authors' views and opinions, neither the European Union nor the European Commission can be considered responsible for them. Additionally, this research was supported by the Italian Ministry of University and Research (MUR) under the PRIN 2022 project titled "Improving the RESilience to climate change of ITalian oak FORests facing dieback (ResItFor)", protocol number 202224ZHWF. AG and JJC would like to acknowledge the financial support from the Spanish Ministry of Science and Innovation and the AEI through projects PID2021-123675OB-C43 and TED2021-129770B-C21. RSS would like to acknowledge the financial support from the Spanish Ministry of Science and Innovation and the AEI through projects PID2021-123675OB-C44 and TED2021-129770B-C22.

Declaration of competing interest

The authors declare that they have no known competing financial interests or personal relationships that could have appeared to influence the work reported in this paper.

Acknowledgments

We extend our gratitude to Pollino National Park, Ticino Regional Park, Gorgoglione and San Paolo Albanese municipalities for permitting us to conduct our research within their experimental areas. We also thank Osvaldo Pericolo for his technical support during the field campaigns and assistance with wood-anatomy measurements. Additionally, we appreciate the Navarra Government for granting us sampling permissions in the Aramendia site.

Appendix A. Supplementary data

Supplementary data to this article can be found online at https://doi.org/10.1016/j.scitotenv.2025.179565.

Data availability

The data supporting the results of this study is publicly available upon request.

References

Alla, A.Q., Camarero, J.J., 2012. Contrasting responses of radial growth and wood anatomy to climate in a Mediterranean ring-porous oak: implications for its future persistence or why the variance matters more than the mean. Eur. J. For. Res. 131, 1537–1550. https://doi.org/10.1007/s10342-012-0621-x.

Allen, C.D., Macalady, A.K., Chenchouni, H., Bachelet, D., McDowell, N., et al., 2010. A global overview of drought and heat-induced tree mortality reveals emerging climate change risks for forests. For. Ecol. Manag. 259, 660–684. https://doi.org/10.1016/j.foreco.2009.09.001.

Amaral Franco, J., 1990. Quercus L. In: Castroviejo, S., Laínz, M., López, G., Montserrat, P., Muñoz, F., Paiva, J., Villar, L. (Eds.), Flora Ibérica. II. Plantas Vasculares de la Península Ibérica e Islas Baleares, RJBM-CSIC, Madrid, pp. 16–36.

Anderegg, W.R., Schwalm, C., Biondi, F., Camarero, J.J., Koch, G., Litvak, M., Ogle, K., Shaw, J.D., Shevliakova, E., Williams, A.P., Wolf, A., Ziaco, E., Pacala, S., 2015. Pervasive drought legacies in forest ecosystems and their implications for carbon cycle models. Science 349 (6247), 528–532. https://doi.org/10.1126/science.aab1833.

Argüelles-Marrón, B., Meave, J.A., Luna-Vega, I., Crispin-DelaCruz, D.B., Szejner, P., Ames-Martínez, F.N., Rodríguez-Ramírez, E.C., 2023. Adaptation potential of Neotropical montane oaks to drought events: Wood anatomy sensitivity in *Quercus delgadoana* and *Quercus meavei*. Funct. Ecol. 37, 2040–2055. https://doi.org/10.1111/1365-2435.14362.

Arnič, D., Gričar, J., Jevšenak, J., Božič, G., von Arx, G., Prislan, P., 2021. Different Wood anatomical and growth responses in European beech (*Fagus sylvatica* L.) at three Forest sites in Slovenia. Front. Plant Sci. 12. https://doi.org/10.3389/fpls.2021.669229.

Borghetti, M., Gentilesca, T., Colangelo, M., Ripullone, F., Rita, A., 2020. Xylem functional traits as indicators of health in Mediterranean forests. Curr Forestry Rep 6, 220–236. https://doi.org/10.1007/s40725-020-00124-5.

Borghetti, M., Gentilesca, T., Leonardi, S., van Noije, T., Rita, A., Mencuccini, M., 2017. Long-term temporal relationships between environmental conditions and xylem functional traits: a meta-analysis across a range of woody species along climatic and nitrogen deposition gradients. Tree Physiol. 37, 4–17. https://doi.org/10.1093/treephys/tpw087.

Bose, A.K., Doležal, J., Scherrer, D., Altman, J., Ziche, D., et al., 2024. Revealing legacy effects of extreme droughts on tree growth of oaks across the northern hemisphere. Sci. Total Environ. 926, 172049. https://doi.org/10.1016/j.scitotenv.2024.172049.

Bréda, N., Huc, R., Granier, A., Dreyer, E., 2006. Temperate forest trees and stands under severe drought: a review of ecophysiological responses, adaptation processes and long-term consequences. Ann. For. Sci. 63 (6), 625–644. https://doi.org/10.1051/forest:2006042.

Cailleret, M., Dakos, V., Jansen, S., Robert, E.M.R., Aakala, T., et al., 2019. Early-warning signals of individual tree mortality based on annual radial growth. Front. Plant Sci. 9. https://doi.org/10.3389/fpls.2018.01964.

Camarero, J.J., Colangelo, M., Gazol, A., Azorín-Molina, C., 2021. Drought and cold spells trigger dieback of temperate oak and beech forests in northern Spain. Dendrochronologia 66, 125812. https://doi.org/10.1016/j.dendro.2021.125812.

Camarero, J.J., Gazol, A., Sangüesa-Barreda, G., Oliva, J., Vicente-Serrano, S., 2015. To die or not to die: early warnings of tree dieback in response to a severe drought. J. Ecol. 103, 44–57. https://doi.org/10.1111/1365-2745.12295.
Carlquist, S., 1977. Ecological factors in wood evolution: a floristic approach. Am. J. Bot. 64, 887–896. https://doi.org/10.1002/j.1537-2197.1977.tb11932.x.
Carlquist, S., 2001. Comparative Wood Anatomy - Systematic, Ecological, and Evolutionary Aspects of Dicotyledon Wood, 2nd edn. Springer Verlag, Berlin.
Castagneri, D., Carrer, M., Regev, L., Boaretto, E., 2020. Precipitation variability differently affects radial growth, xylem traits and ring porosity of three Mediterranean oak species at xeric and Mesic sites. Sci. Total Environ. 699, 134285. https://doi.org/10.1016/j.scitotenv.2019.134285.
Castellaneta, M., Rita, A., Camarero, J.J., Colangelo, M., Ripullone, F., 2022. Declines in canopy greenness and tree growth are caused by combined climate extremes during drought-induced dieback. Sci. Total Environ. 2022 (813), 152666. https://doi.org/10.1016/j.scitotenv.2021.152666.
Clark, P.J., Evans, F.C., 1954. Distance to nearest neighbour as a measure of spatial relationships in populations. Ecology 35, 445–453. https://doi.org/10.2307/1931034.
Colangelo, M., Camarero, J.J., Battipaglia, G., Borghetti, M., De Micco, V., Gentilesca, T., Ripullone, F., 2017a. A multi-proxy assessment of dieback causes in a Mediterranean oak species. Tree Physiol. 37, 617–631. https://doi.org/10.1093/treephys/tpx002.
Colangelo, M., Camarero, J.J., Borghetti, M., Gazol, A., Ripullone, F., 2017. Size matters a lot: drought-affected Italian oaks are smaller and show lower growth prior to tree death. Front. Plant Sci. 8, 135. https://doi.org/10.3389/fpls.2017.00135.
Colangelo, M., Camarero, J.J., Borghetti, M., Gentilesca, T., Oliva, J., Redondo, M.A., Ripullone, F., 2018b. Drought and *Phytophthora* are associated with the decline of oak species in southern Italy. Front. Plant Sci. 9, 1595. https://doi.org/10.3389/fpls.2018.01595.
Colangelo, M., Camarero, J.J., Ripullone, F., Gazol, A., Sánchez-Salguero, R., Oliva, J., Redondo, M.A., 2018a. Drought decreases growth and increases mortality of coexisting native and introduced tree species in a temperate floodplain forest. Forests 9, 205. https://doi.org/10.3390/f9040205.
Corcuera, L., Camarero, J.J., Gil-Pelegrín, E., 2004. Effects of a severe drought on growth and wood-anatomical properties of *Quercus faginea*. IAWA J. 25, 185–204. https://doi.org/10.1163/22941932-90000360.
Cornes, R.C., Van der Schier, G., van den Besselar, E.J.M., Jones, P.D., 2018. An ensable version of the E-OBS temperature and precipitation data sets. J. Geophys. Res. Atmos. 123, 9391–9409. https://doi.org/10.1029/2017J D028200.
Damesin, C., Rambal, S., 1995. Field study of leaf photosynthetic performance by a Mediterranean deciduous oak tree (*Quercus pubescens*) during a severe summer drought. New Phytol. 131, 159–167. https://doi.org/10.1111/j.1469-8137.1995.tb05717.x.
DEPFAR, 2026. Indagini Diagnostiche sul Deperimento Della Farina nei Boschi Della Valle del Ticino. Consorzio Parco Lombardo della Valle del Ticino, Pontevecchio di Magenta, Italy.
DeSoto, L., Cailleret, M., Sterck, F., Jansen, S., Kramer, K., Robert, E.M., et al., 2020. Low growth resilience to drought is related to future mortality risk in trees. Nat. Commun. 11, 545. https://doi.org/10.1038/s41467-020-14300-5.
Di Pietro, R., Conte, A.L., Di Marzio, P., Gianguzzi, L., Spampinato, G., Caldarella, O., Fortini, P., 2020. A multivariate morphometric analysis of diagnostic traits in southern Italy and Sicily pubescent oaks. Folia Geobot. 55, 163–183. https://doi.org/10.1007/s12224-020-09378-0.
Dobbertin, M., 2005. Tree growth as indicator of tree vitality and of tree reaction to environmental stresses: a review. Eur. J. For. Res. 124, 319–333. https://doi.org/10.1007/s10342-005-0085-3.
Epron, D., Dreyer, E., 1993. Long-term effects of drought on photosynthesis of adult oak trees [*Quercus petraea* (Matt.) Liebl. And *Quercus robur* L.] in a natural stand. New Phytol. 125, 381–389. https://doi.org/10.1111/j.1469-8137.1993.tb03890.x.
Fonti, P., García-González, I., 2008. Earlywood vessel size of oak as a potential proxy for spring precipitation in Mesic sites. J. Biogeogr. 35, 2249–2257. https://doi.org/10.1111/j.1365-2699.2008.01961.x.
Fonti, P., von Arx, G., García-González, I., Eilmann, B., Sass-Klaassen, U., Gärtner, H., Eckstein, D., 2010. Studying global change through investigation of the plastic responses of xylem anatomy in tree rings. New Phytol. 185 (1), 42–53. https://doi.org/10.1111/j.1469-8137.2009.03030.x.
Fritts, H.C., 1976. Tree Rings and Climate. Academic Press, London.
García-González, I., Eckstein, D., 2003. Climatic signal of earlywood vessels of oak on a maritime site. Tree Physiol. 23, 497–504. https://doi.org/10.1093/treephys/23.7.497.
Gärtner, H., Nievergelt, D., 2010. The core-microtome: a new tool for surface preparation on cores and time series analysis of varying cell parameters. Dendrochronologia 28, 85–92. https://doi.org/10.1016/j.dendro.2009.09.002.
Gazol, A., Camarero, J.J., Sánchez-Salguero, R., Vicente-Serrano, S.M., Serra-Maluquer, X., et al., 2020. Drought legacies are short, prevail in dry conifer forests and depend on growth variability. J. Ecol. 108, 2473–2484. https://doi.org/10.1111/1365-2745.13435.
Gea-Izquierdo, G., Fonti, P., Cherubini, P., Martín-Benito, D., Chaar, H., Cañellas, I., 2012. Xylem hydraulic adjustment and growth response of *Quercus canariensis* Willd. To climatic variability. Tree Physiol. 32, 401–403. https://doi.org/10.1093/treephys/tps026.
Gentilesca, T., Camarero, J.J., Colangelo, M., Nolã, A., Ripullone, F., Nole, A., 2017. Drought-induced oak decline in the western Mediterranean region: an overview on current evidences, mechanisms and management options to improve forest resilience. iForest 10, 796–806. https://doi.org/10.3832/ifor2317-010.
Granda, E., Alla, A.Q., Laskurain, N.A., Loidi, J., Sánchez-Lorenzo, A., Camarero, J.J., 2017. Coexisting oak species, including rear-edge populations, buffer climate stress through xylem adjustments. Tree Physiol. 38, 159–172. https://doi.org/10.1093/treephys/tpx157.
Gričar, J., De Luis, M., Hafner, P., Levanič, T., 2013. Anatomical characteristics and hydrologic signals in tree-rings of oaks (*Quercus robur* L.). Trees 27, 1669–1680. https://doi.org/10.1007/s00468-013-0914-9.
Guada, G., Sass-Klaassen, U., Souto-Herrero, M., García-González, I., 2021. Anatomical tree-ring chronologies and seasonal patterns of cambial dynamics are valuable indicators of tree performance of two oak species at the Atlantic-Mediterranean boundary. Dendrochronologia 70, 125893. https://doi.org/10.1016/j.dendro.2021.125893.
Guada, G., Vázquez-Ruiz, R.A., García-González, I., 2019. Response patterns of xylem and leaf phenology to temperature at the southwestern distribution boundary of *Quercus robur*: a multi-spatial study. Agric. For. Meteorol. 269, 46–56. https://doi.org/10.1016/j.agrformet.2019.02.001.
Hochberg U., Rockwell F.E., Holbrook N.M, Cochard H. 2018. Iso/Anisohydry: A Plant–Environment Interaction Rather Than a Simple Hydraulic Trait. Trends Plant Sci., 23 (2): 112–120. https://doi.org/10.1016/j.tplants.2017.11.002.
Holmes, R.L., 1983. Computer-assisted quality control in tree-ring dating and measurement. Tree-Ring Bull. 43, 69–78.
Kahmen, A., Basler, D., Hoch, G., Link, R.M., Schuldt, B., Zahnd, C., Arend, M., 2022. Root water uptake depth determines the hydraulic vulnerability of temperate European tree species during the extreme 2018 drought. Plant Biol. 24, 1224–1239. https://doi.org/10.1111/plb.13476.
Klein, T., 2014. The variability of stomatal sensitivity to leaf water potential across tree species indicates a continuum between isohydric and anisohydric behaviours. Funct. Ecol. 28, 1313–1320.
Levanič, T., Čater, M., McDowell, N.G., 2011. Associations between growth, wood anatomy, carbon isotope discrimination and mortality in a *Quercus robur* forest. Tree Physiol. 31, 298–308. https://doi.org/10.1093/treephys/tpq111.
Marchand, L.J., Dox, I., Gričar, J., et al., 2021. Timing of spring xylogenesis in temperate deciduous tree species relates to tree growth characteristics and previous autumn phenology. Tree Physiol. 41, 1161–1170. https://doi.org/10.1093/treephys/tpaa171.
Martínez-Vilalta, J., Mencuccini, M., Álvarez, X., Camacho, J., Loepfe, L., Piñol, J., 2012. Spatial distribution and packing of xylem conduits. Am. J. Bot. 99, 1189–1196. https://doi.org/10.3732/ajb.1100384.
McDowell, N.G., Beerling, D.J., Breshears, D.D., Fisher, R.A., Raffa, K.F., Stitt, M., 2011. The interdependence of mechanisms underlying climate-driven vegetation mortality. Trends Ecol. Evol. 26 (10), 523–532. https://doi.org/10.1016/j.tree.2011.06.003.
Mencuccini, M., Martinez-Vilalta, J., Piñol, J., Loepfe, L., Burnat, M., Alvarez, X., Camacho, J., Gil, D., 2010. A quantitative and statistically robust method for the determination of xylem conduit spatial distribution†. Am. J. Bot. 97, 1247–1259. https://doi.org/10.3732/ajb.0900289.
Michelot, A., Simard, S., Rathgeber, C., Dufrêne, E., Damesin, C., 2012. Comparing the intra-annual wood formation of three European species (*Fagus sylvatica*, *Quercus petraea* and *Pinus sylvestris*) as related to leaf phenology and non-structural carbohydrate dynamics. Tree Physiol. 32, 1033–1045. https://doi.org/10.1093/treephys/tps052.
Nardini, A., Battistuzzo, M., Savi, T., 2013. Shoot desiccation and hydraulic failure in temperate woody angiosperms during an extreme summer drought. New Phytol. 200, 322–329. https://doi.org/10.1111/nph.12288.
Nola, P., Bracco, F., Assini, S., von Arx, G., Castagneri, D., 2020. Xylem anatomy of *Robinia pseudoacacia* L. and *Quercus robur* L. is differently affected by climate in a temperate alluvial forest. Ann. For. Sci. 77, 8. https://doi.org/10.1007/s13595-019-0906-z.
Olson, M.E., Anfodillo, T., Rosell, J.A., Petit, G., Crivellaro, A., Isnard, S., León- Gómez, J. A., Alvarado-Cárdenas, L.O., Castorena, M., 2014. Universal hydraulics of the flowering plants: vessel diameter scales with stem length across angiosperm lineages, habits and climates. Ecol. Lett. 17, 988–997. https://doi.org/10.1111/ele.12302.
Pellizzari, E., Camarero, J.J., Gazol, A., Sangüesa-Barreda, G., Carrer, M., 2016. Wood anatomy and carbon-isotope discrimination support long-term hydraulic deterioration as a major cause of drought-induced dieback. Glob. Chang. Biol. 22, 2125–2137. https://doi.org/10.1111/gcb.13227.
Pérez-de-Lis, G., Rozas, V., Vázquez-Ruiz, R.A., García-González, I., 2018. Do ring-porous oaks prioritize earlywood vessel efficiency over safety? Environmental effects on vessel diameter and tyloses formation. Agric. For. Meteorol. 248, 205–214. https://doi.org/10.1016/j.agrformet.2017.09.022.
Pericolo, O., Camarero, J.J., Colangelo, M., Valeriano, C., Sánchez-Salguero, R., et al., 2023. Species-specific vulnerability to increased drought in temperate and Mediterranean floodplain forests. Agric. For. Meteorol. 328, 109238. https://doi.org/10.1016/j.agrformet.2022.109238.
Pinheiro, J., Bates, D., R Core Team, 2023. Nlme: linear and nonlinear mixed effects models. R package version 3, 1–162. https://CRAN.R-project.org/package=nlme.
Pinheiro, J.C., Bates, D.M., 2000. Mixed-Effects Models in S and S-PLUS. Springer, New York.
Preisler, Y., Tatarinov, F., Grünzweig, J.M., Yakir, D., 2021. Seeking the "point of no return" in the sequence of events leading to mortality of mature trees. Plant Cell Environ. 44, 1315–1328. https://doi.org/10.1111/pce.13942.
R Core Team, 2024. R: A Language and Environment for Statistical Computing. R Foundation for Statistical Computing, Vienna, Austria.
Ripullone, F., Camarero, J.J., Colangelo, M., Voltas, J., 2020. Variation in the access to deep soil water pools explains tree-to-tree differences in drought-triggered dieback of Mediterranean oaks. Tree Physiol. 40, 591–604. https://doi.org/10.1093/treephys/tpaa026.
Roman, D.T., Novick, K.A., Brzostek, E.R., Dragoni, D., Rahman, F., Phillips, R.P., 2015. The role of isohydric and anisohydric species in determining ecosystem-scale

response to severe drought. Oecologia 179, 641–654. https://doi.org/10.1007/s00442-015-3380-9.
Sánchez-Salguero, R., Camarero, J.J., Gutiérrez, E., González Rouco, F., Gazol, A., Sangüesa-Barreda, G., Andreu-Hayles, L., Linares, J.C., Seftigen, K., 2017. Assessing forest vulnerability to climate warming using a process-based model of tree growth: bad prospects for rear-edges. Glob. Chang. Biol. 23, 2705–2719. https://doi.org/10.1111/gcb.13541.
Sánchez-Salguero, R., Colangelo, M., Matías, L., Ripullone, F., Camarero, J.J., 2020. Shifts in growth responses to climate and exceeded drought-vulnerability thresholds characterize dieback in two Mediterranean deciduous oaks. Forests 11, 714. https://doi.org/10.3390/f11070714.
Sass-Klaassen, U., Fonti, P., Cherubini, P., Grièar, J., Robert, E.M., Steppe, K., Bräuning, A., 2011. A tree-centered approach to assess impacts of extreme climatic events on forests. Front. Plant Sci. 7, 1069. https://doi.org/10.3389/fpls.2016.01069.
Schneider, C., Rasband, W., Eliceiri, K., 2012. NIH image to ImageJ: 25 years of image analysis. Nat. Methods 9, 671–675. https://doi.org/10.1038/nmeth.2089.
Scholz, A., Klepsch, M., Karimi, Z., Jansen, S., 2013. How to quantify conduits in wood? Front. Plant Sci. 4. https://doi.org/10.3389/fpls.2013.00056.
Serrano, M.S., Romero, M.A., Homet, P., Gómez-Aparicio, L., 2022. Climate change impact on the population dynamics of exotic pathogens: the case of the worldwide pathogen *Phytophthora cinnamomi*. Agric. For. Meteorol. 322, 109002. https://doi.org/10.1016/j.agrformet.2022.109002.
Skiadaresis, G., Schwarz, J.A., Bauhus, J., 2019. Groundwater extraction in floodplain forests reduces radial growth and increases summer drought sensitivity of pedunculate oak trees (*Quercus robur* L.). Frontiers in forests and global. Change 2, 5. https://doi.org/10.3389/ffgc.2019.00005.
Sperry, J.S., Nichols, K.L., Sullivan, J.E.M., Eastlack, S.E., 1994. Xylem embolism in ring-porous, diffuse-porous, and coniferous trees in northern Utah and interior Alaska. Ecology 75, 1736–1752. https://doi.org/10.2307/1939633.
Süßel, F., Brüggemann, W., 2021. Properties of secondary xylem of mature oaks in Southwest Germany formed after extreme drought stress in summer 2018. Trees, Forests and People 5, 100097. https://doi.org/10.1016/j.tfp.2021.100097.
Valeriano, C., Gazol, A., Colangelo, M., Camarero, J.J. 2021b. Drought Drives Growth and Mortality Rates in Three Pine Species under Mediterranean Conditions. Forests 2021, 12, 1700. https://doi.org/10.3390/f12121700.
Valeriano, C., Gazol, A., Colangelo, M., González de Andrés, E., Camarero, J.J., 2021. Modeling climate impacts on tree growth to assess tree vulnerability to drought during Forest dieback. Front. Plant Sci. 12, 672855. https://doi.org/10.3389/fpls.2021.672855.
Van der Werf, G.W., Sass-Klaassen, U.G., Mohren, G.M.J., 2007. The impact of the 2003 summer drought on the intra-annual growth pattern of beech (*Fagus sylvatica* L.) and oak (*Quercus robur* L.) on a dry site in the Netherlands. Dendrochronologia 25, 103–112. https://doi.org/10.1016/j.dendro.2007.03.004.
Vicente-Serrano, S.M., Beguería, S., López-Moreno, J.I., 2010. A multiscalar drought index sensitive to global warming: the standardized precipitation evapotranspiration index. J. Clim. 23, 1696–1718. https://doi.org/10.1175/2009JCLI2909.1.
Wood, S.N., 2003. Thin plate regression splines. Journal of the Royal Statistical Society B 65, 95–114. https://doi.org/10.1111/1467-9868.00374.
Wood, S.N., 2011. Fast stable restricted maximum likelihood and marginal likelihood estimation of semiparametric generalized linear models. Journal of the Royal Statistical Society B 73, 3–36. https://doi.org/10.1111/j.1467-9868.2010.00749.x.
Wood, S.N., 2017. Generalized additive models: an introduction with R. CRC Press. https://doi.org/10.1201/9781315370279.
Zhang, X., Li, Q., Yang, Y., Fukuda, K., Morris, H., Jansen, S., Da, L., Song, K., 2024. A higher tissue fraction of parenchyma in secondary xylem supports growth recovery of angiosperm trees after drought. Funct. Ecol. 38, 2709–2719. https://doi.org/10.1111/1365-2435.14680.
Zomer, R.J., Xu, J., Trabucco, A., 2022. Version 3 of the global aridity index and potential evapotranspiration database. Sci Data 9, 409. https://doi.org/10.1038/s41597-022-01493-1.